NeuroImage: Clinical 33 (2022) 102951

Contents lists available at ScienceDirect

NeuroImage: Clinical

journal homepage: www.elsevier.com/locate/ynicl

Anterior precuneus related to the recovery of consciousness

Hang Wu [a,1], Zengxin Qi [b,c,d,1], Xuehai Wu [b,c,d,e,1], Jun Zhang [f], Changwei Wu [g,h,i], Zirui Huang [j], Di Zang [b,c,d], Stuart Fogel [k], Sean Tanabe [j], Anthony G. Hudetz [j], Georg Northoff [l,m], Ying Mao [b,c,d,*], Pengmin Qin [a,e,*]

[a] Key Laboratory of Brain, Cognition and Education Sciences, Ministry of Education, School of Psychology, Center for Studies of Psychological Application, and Guangdong Key Laboratory of Mental Health and Cognitive Science, South China Normal University, Guangzhou, Guangdong 510631, China
[b] Department of Neurosurgery, Huashan Hospital, Shanghai Medical College, Fudan University, Shanghai 200433, China
[c] Neurosurgical Institute of Fudan University, Shanghai Clinical Medical Center of Neurosurgery, Shanghai Key Laboratory of Brain Function Restoration and Neural Regeneration, Shanghai 200433, China
[d] State Key Laboratory of Medical Neurobiology and MOE Frontiers Center for Brain Science, School of Basic Medical Sciences and Institutes of Brain Science, Fudan University, Shanghai 200433, China
[e] Pazhou Lab, Guangzhou 510335, China
[f] Department of Anesthesiology, Fudan University Shanghai Cancer Center Shanghai, 200433, China
[g] Research Center for Brain and Consciousness, Taipei Medical University, Taipei 11031, Taiwan
[h] Graduate Institute of Humanities in Medicine, Taipei Medical University, Taipei 11031, Taiwan
[i] Shuang-Ho Hospital, Taipei Medical University, New Taipei 23561, Taiwan
[j] Department of Anesthesiology and Center for Consciousness Science, University of Michigan, Ann Arbor, MI 48105, USA
[k] School of Psychology, University of Ottawa, Ottawa, ON K1N 6N5, Canada
[l] Institute of Mental Health Research, University of Ottawa, Ottawa, Ontario, ON K1Z 7K4, Canada
[m] Mental Health Centre, Zhejiang University School of Medicine, Hangzhou 310058, China

ARTICLE INFO

Keywords:
Recovery of consciousness
Unresponsive wakefulness syndrome
Anesthesia
N3 sleep
Degree centrality
Anterior precuneus

ABSTRACT

The neural mechanism that enables the recovery of consciousness in patients with unresponsive wakefulness syndrome (UWS) remains unclear. The aim of the current study is to characterize the cortical hub regions related to the recovery of consciousness. In the current fMRI study, voxel-wise degree centrality analysis was adopted to identify the cortical hubs related to the recovery of consciousness, for which a total of 27 UWS patients were recruited, including 13 patients who emerged from UWS (UWS-E), and 14 patients who remained in UWS (UWS-R) at least three months after the experiment performance. Furthermore, other recoverable unconscious states were adopted as validation groups, including three independent N3 sleep datasets (n = 12, 9, 9 respectively) and three independent anesthesia datasets (n = 27, 14, 6 respectively). Spatial similarity of the hub characteristic with the validation groups between the UWS-E and UWS-R was compared using the dice coefficient. Finally, with the cortical regions persistently shown as hubs across UWS-E and validation states, functional connectivity analysis was further performed to explore the connectivity patterns underlying the recovery of consciousness. The results identified four cortical hubs in the UWS-E, which showed significantly higher degree centrality for UWS-E than UWS-R, including the anterior precuneus, left inferior parietal lobule, left inferior frontal gyrus, and left middle frontal gyrus, of which the degree centrality value also positively correlated with the patients' Glasgow Outcome Scale (GOS) score that assessed global brain functioning outcome after a brain injury. Furthermore, the anterior precuneus was found with significantly higher similarity of hub characteristics as well as functional connectivity patterns between UWS-E and the validation groups. The results suggest that the recovery of consciousness may be relevant to the integrity of cortical hubs in the recoverable unconscious states, especially the anterior precuneus. The identified cortical hub regions could serve as potential treatment targets for patients with UWS.

* Corresponding authors at: Neurosurgical Department, Shanghai Huashan Hospital, Fudan University, Shanghai 200433, China. Centre for Studies of Psychological Applications, Guangdong Key Laboratory of Mental Health and Cognitive Science, School of Psychology, South China Normal University, Guangzhou, Guangdong 510631, China.
E-mail addresses: maoying@fudan.edu.cn (Y. Mao), qin.pengmin@m.scnu.edu.cn (P. Qin).
[1] These authors contributed equally to this work.

https://doi.org/10.1016/j.nicl.2022.102951
Received 21 September 2021; Received in revised form 22 January 2022; Accepted 25 January 2022
Available online 30 January 2022
2213-1582/© 2022 The Author(s). Published by Elsevier Inc. This is an open access article under the CC BY-NC-ND license (http://creativecommons.org/licenses/by-nc-nd/4.0/).

1. Introduction

Disorders of consciousness (DOC) are usually due to severe brain damage, which includes unresponsive wakefulness syndrome (UWS) and minimally conscious state (MCS) (Giacino et al., 2014). Of all UWS patients, some could eventually regain consciousness, and some don't (Laureys et al., 2010). The identification of robust prognostic markers for the recovery of consciousness in UWS has significant values in the fields of clinical and basic researches (Edlow et al., 2020). Due to the lack of behavioral responsiveness in patients with DOC (Song et al., 2018), resting-state fMRI (rs-fMRI) was broadly used to detect residual consciousness in patients with DOC by measuring the brain connection within large-scale brain networks (Amico et al., 2017; Qin et al., 2021; Rosazza et al., 2016), providing a potential approach to predict their recovery of consciousness (Qin et al., 2015; Silva et al., 2015).

Graph theory is one of the methods that has been applied in studying the connection within or between brain networks for patients with DOC (Achard et al., 2012; Malagurski et al., 2019), since cortical regions with high functional integration with other regions could play a crucial role in supporting consciousness (Luppi et al., 2019; Northoff and Huang, 2017; Northoff and Lamme, 2020). In the graph theoretical analysis, these cortical regions were defined as cortical hubs (Bullmore and Sporns, 2009; Heuvel et al., 2011). Degree centrality is a common metric developed based on graph theory (Wang et al., 2011), in which a higher degree centrality value reflects a larger number of connections between a node (voxel) and the rest of the nodes in the brain (Sporns et al., 2007), and a cluster of nodes with high degree centrality values is considered a hub. Previous studies using this method have found interesting results, for instance, cortical hubs were found to be largely reorganized in DOC patients compared to fully conscious volunteers (Achard et al., 2012; Malagurski et al., 2019). More importantly, some studies have found similar cortical hub distributions among DOC and other recoverable unconscious states, such as N3 sleep and anesthesia (Luppi et al., 2019). These findings lead to the assumption that cortical hubs were essential for supporting the recovery of consciousness. Furthermore, a recent study has showed that cortical hub regions involved in sensorimotor integration were crucial for consciousness (Qin et al., 2021). Following these threads, we came to the hypothesis that cortical hubs related to sensorimotor integration might also play an important role in the recovery of consciousness, which, however, remains to be investigated.

In the current study, we aim to identify the cortical hubs that could support the recovery of consciousness by comparing the difference and similarity in the distribution of cortical hubs across UWS patients who recover consciousness after 3 months and those who do not, as well as other recoverable unconscious states (N3 sleep and anesthesia state). For that purpose, we recruited two subgroups of UWS patients: patients who emerged from UWS (UWS-E) and patients who remained in UWS (UWS-R) at least three months after the experiment performance. Two recoverable unconscious states were used as validation groups (including three independent groups of N3 sleep and three independent groups of anesthesia state), to compare their similarity of the spatial distribution of hubs with UWS patients. Specifically, we first conducted the degree centrality analysis on the two subgroups of UWS patients. After obtaining hub regions (defined as regions of interest, ROI) that play a crucial role in differentiating the two groups, the dice coefficient was then used to assess the similarity between the spatial distribution of hubs in UWS-E and the validation groups (N3 sleep and anesthesia states), as well as UWS-R and the validation groups within these ROIs, respectively. Finally, the common cortical hubs across UWS-E, N3 sleep, and anesthesia groups were used as seeds, and seed-based functional connectivity was calculated to explore the corresponding brain network related to the recovery of consciousness.

2. Materials and methods

2.1. Participants and imaging acquisitions: UWS patients

This dataset included thirty-one UWS patients, in which 21 of them were previously used for a different purpose in a published study (Qin et al., 2015), and 10 patients were newly added in the current study. In the current study, all patients were recruited from Huashan Hospital affiliated to Fudan University (Shanghai, China). Informed written consent was obtained from the legal representatives of the patients, and the study was approved by the Ethics Committee of Huashan Hospital. Due to excessive head motion, four patients were excluded from subsequent analysis, leaving twenty-seven patients (male/female: 20/7; age range: 17–67 years) with structurally well-preserved brain images, which were carefully chosen by author XW and checked by author PQ. In the same day, before the fMRI scanning, the behavioral responsiveness of the UWS patients was assessed with the Coma Recovery Scale-Revised (CRS-R) scale (Giacino et al., 2004). The patients were assessed again at least 3 months after the scanning using the Glasgow Outcome Scale (GOS). In the current study, eight patients with a GOS score of 3 ("Severe disability") and five patients with a score of 4 ("Moderate disability") were regarded as emerged from UWS (UWS-E, male/female: 9/4; age range: 17–52 years; number of patients for different age groups: 17–26 years: 2 patients, 27–36 years: 1 patients, 37–46 years: 9 patients, 47–56 years: 1 patients), and 14 patients with a GOS score equals to 2 ("Persistent vegetative state") were regarded as remained in UWS (UWS-R, male/female: 11/3; age range: 26–67 years; number of patients for different age groups: 17–26 years: 1 patients, 27–36 years: 2 patients, 37–46 years: 2 patients, 47–56 years: 5 patients, 57–67 years: 4 patients). Thus, each patient was assigned to one of the two subgroups (UWS-E or UWS-R) according to his/her GOS score, and the following data analysis as well as statistic comparison were performed based on the two subgroups. In addition, no significant difference was found between UWS-E and UWS-R in terms of sex ($p = 0.58$), age ($p = 0.07$), days after insult ($p = 0.73$), or CRS-R score at the time of scan ($p = 0.98$) (See Table 1 for detailed demographic and clinical information). To see the effects of etiology, a chi-square test was performed, and showed a p value = 0.15.

In this dataset, the MR images were acquired using a Siemens 3 Tesla scanner. Functional images were acquired using a T2*-weighted EPI sequence (TR/TE/θ = 2000 ms/35 ms/90°, FOV = 256 × 256 mm, matrix = 64 × 64, 33 slices with 4-mm thickness, gap = 0 mm, 200 scans). For functional image registration and localization, a high-resolution T1-weighted anatomical image was also acquired for each participant.

2.2. Participants and imaging acquisitions: Sleep and anesthesia groups

In order to validate the results obtained from the UWS groups, additional recoverable unconscious states were collected, including the anesthesia and N3 sleep state. Specifically, for repeatability validation, three independent datasets of N3 sleep and three of anesthesia were included. In addition, to measure the behavioral responsiveness for each participant, behavioral assessment was used for the anesthesia groups, and EEG signal was used for the N3 sleep groups. For detailed demographic information of each validation group, please see Supplementary Table 1.

2.2.1. Sleep group 1

This dataset was analyzed for a different purpose in a previously published study (Tsai et al., 2014). Twelve healthy men (ages 20 to 27) were included, who slept for 7–8 h each night and had a consistent bed/wake time for four days. Informed consents were obtained from all participants, and ethical approval was obtained from the Institutional Review Board of National Yang-Ming University. For the sleep protocol, simultaneous EEG–fMRI was recorded. The sleep protocol was

Table 1
Demographic and clinical information for unresponsive wakefulness syndrome patients.

Patient number	Sex/ Age	Cause	Time of fMRI (days after insult)	CRS-R	Diagnosis	GOS
p1	F/35	TBI	21	5	UWS-E	4
p2	F/24	TBI	1	3	UWS-E	4
p3	M/46	SIH	18	2	UWS-E	4
p4	F/43	SIH	162	6	UWS-E	3
p5	M/52	TBI	210	6	UWS-E	3
p6	M/38	TBI	81	3	UWS-E	3
p7	M/46	TBI	25	2	UWS-E	3
p8	M/44	TBI	21	3	UWS-E	4
p9	F/39	TBI	31	6	UWS-E	3
p10	M/45	TBI	12	6	UWS-E	4
p11	M/46	TBI	168	1	UWS-E	3
p12	M/46	TBI	162	5	UWS-E	3
p13	M/17	Anoxic	493	7	UWS-E	3
p14	M/50	TBI	137	3	UWS-R	2
p15	M/30	TBI	259	8	UWS-R	2
p16	F/57	TBI	15	3	UWS-R	2
p17	M/60	SIH	109	6	UWS-R	2
p18	M/26	TBI	143	6	UWS-R	2
p19	M/47	SIH	315	6	UWS-R	2
p20	M/46	Anoxic	23	3	UWS-R	2
p21	M/51	TBI	100	4	UWS-R	2
p22	M/53	TBI	30	3	UWS-R	2
p23	F/67	TBI	10	3	UWS-R	2
p24	M/57	SIH	33	2	UWS-R	2
p25	F/52	SIH	51	4	UWS-R	2
p26	M/39	SIH	221	4	UWS-R	2
p27	M/35	SIH	300	4	UWS-R	2

Note: UWS = unresponsive wakefulness syndrome; UWS-E = patients who emerged from UWS at least three months after the experiment performance; UWS-R = patients who remained in UWS at least three months after the experiment performance; CRS-R = Coma Recovery Scale-Revised; GOS = Glasgow Outcome Scale; SIH = spontaneous intracerebral hemorrhage; TBI = traumatic brain injury.

conducted at midnight and the participants were told to try to fall asleep as soon as the EPI scan began. A licensed sleep technician at Kaohsiung Medical University Hospital visually rated sleep stages for every 30-second, according to the American Academy of Sleep Medicine's current criteria (AASM).

The MR images were acquired on a 3 Tesla Siemens Tim-Trio scanner. Functional images were acquired using a T2*-weighted EPI sequence (TR/TE/θ = 2500 ms/30 ms/80°, FOV = 220 × 220 mm, matrix = 64 × 64, 35 slices with 3.4 mm thickness). A high-resolution T1-weighted anatomical image was acquired on each participant for functional image registration and localization. More details on the EEG and fMRI data acquisition parameters and preprocessing can be found in the previous analysis (Tsai et al., 2014).

2.2.2. Sleep group 2

The dataset was analyzed for a different purpose in a previously published study (Fang et al., 2019). In the current study, nine healthy participants with a persistent N3 sleep stage (male/female: 3/6; age range: 18–33 years) were included using simultaneous EEG–fMRI recordings. Informed consents were obtained from all participants and ethical approval was obtained from the Health Science research ethics board of Western University. The sleep stages were scored in the same way as Sleep group 1. The MR images were acquired on a 3 Tesla Siemens Magnetom Prisma scanner. Functional images were acquired using a T2*-weighted EPI sequence (TR/TE/θ = 2160 ms/30 ms/90°, FOV = 220 × 220 mm, matrix = 64 × 64 × 40, 40 slices with 3 mm thickness). For image registration and localization, a high-resolution T1-weighted anatomical image was acquired for each participant. More details about the EEG and fMRI data acquisition parameters and data preprocessing can be found in the previous analysis (Fang et al., 2019).

2.2.3. Sleep group 3

The dataset was analyzed for a different purpose in a previously published study (Fogel et al., 2017). Nine healthy participants (male/female: 5/4; age range: 22–35 years) with a persistent N3 sleep stage were included. Informed consents were obtained from all participants and ethical approval was obtained from the Research Ethics Board at the Institut universitaire de gériatrie de Montréal (IUGM). The sleep stages were scored in the same way as Sleep group 1 and Sleep group 2 using simultaneous EEG–fMRI recordings. MR images were acquired on a 3 Tesla Siemens Tim-Trio scanner. Functional images were acquired using a T2*-weighted EPI sequence (TR/TE/θ = 2160 ms/30 ms/90°, FOV = 220 mm, matrix size = 64 × 64, slice thickness = 3 mm, 40 slices). A high-resolution T1-weighted anatomical image was acquired for each participant for image registration and localization. More details on the EEG and fMRI data acquisition parameters and preprocessing can be found in the previous analysis (Fogel et al., 2017).

2.2.4. Anesthesia group 1

The dataset was analyzed for a difference purpose in a previously published study (Huang et al., 2014). Twenty-seven participants received intravenous propofol anesthesia (male/female: 13/14; age range: 27–64 years). The elective transsphenoidal approach for resection of pituitary microadenoma had been used on all the participants. An informed written consent was obtained from each participant, and the study was approved by the Ethics Committee of Shanghai Huashan Hospital, Fudan University, Shanghai, China.

A plasma concentration of 3.0–5.0 μg/ml was achieved using a target-controlled infusion (TCI) based on the Marsh model. Unconsciousness was reliably induced using TCI propofol at a stable effect-site concentration (4.0 μg/ml) for each participant. A participant was considered unconscious (Ramsay 5–6) if he/she did not respond to verbal commands such as "squeeze my hand" during anesthesia. Furthermore, in the post-operative follow-up, no participant reported explicit recollection. Therefore, all participants were deemed unconscious during anesthesia. Participants were given intermittent positive pressure ventilation during the anesthetic state, with a tidal volume of 8–10 ml/kg, a respiratory rate of 10–12 beats per minute, and a PetCO2 (end tidal partial pressure of CO2) of 35–37 mmHg. Throughout the study, two certified anesthesiologists were present to ensure the accessibility of resuscitation equipment. See the previous study for more details of the anesthesia protocols (Huang et al., 2014).

A Siemens 3 T scanner (Siemens, Erlangen, Germany) was used to obtain functional images of the whole brain using a T2*-weighted EPI series (TR/TE/θ = 2000 ms/30 ms/90°, FOV = 192 mm, matrix size = 64 × 64, 25 slices with 6-mm thickness, gap = 0 mm, 240 scans). A high-resolution T1-weighted anatomical image was acquired for each participant for functional image registration and localization.

2.2.5. Anesthesia group 2

The dataset was analyzed for a difference purpose in a previously published study (Liu et al., 2017). One participant was excluded due to excessive head motion, leaving fourteen participants (male/female: 8/6; age range: 19–34 years) in the current study. An informed written consent was obtained from each participant and the study was approved by the Ethics Committee of Medical College of Wisconsin (MCW).

The levels of behavioral responsiveness were measured using the OAAS (observer's assessment of alertness/sedation). Participants responded readily to verbal commands during baseline conscious and recovery conditions (OAAS score, 5). Participants responded to verbal commands with a sluggishness when under light sedation (OAAS score, 4). During deep sedation, participants showed no response to verbal instruction (OAAS score, 2 and 1). The resulting target plasma concentrations differ among participants (light sedation, 0.98 ± 0.18 μg/ml; deep sedation, 1.88 ± 0.24 μg/ml) due to the variability of individual anesthetic susceptibility. During anesthesia, the plasma concentration of propofol was maintained in equilibrium by constantly changing the

infusion rate to maintain the balance between accumulation and drug elimination. The infusion rate was manually monitored and driven by the results of a computer simulation based on the pharmacokinetic model of propofol that was designed for target-controlled drug infusion (STANPUMP). During the procedure, the electrocardiogram, noninvasive blood pressure cuff, pulse oximetry, and end-tidal carbon dioxide gas monitoring were all performed according to the standard American Society of Anesthesiologists (ASA) protocols. A nasal cannula was used to administer supplemental oxygen as a preventative measure. For more details on the anesthesia procedures, see the previous studies (Liu et al., 2017).

Functional images of the whole brain were acquired using a 3 T Signa GE 750 scanner (GE Healthcare, Waukesha, WI, USA) that used T2*-weighted EPI sequence (TR/TE/θ = 2000 ms/25 ms/77°, FOV = 224 mm, matrix size = 64 × 64, 41 slices with 3.5 mm thickness, 450 scans). A high-resolution T1-weighted anatomical image was acquired for each participant for image registration and localization.

2.2.6. Anesthesia group 3

The dataset was analyzed for a difference purpose in a previously published study (Huang et al., 2014). Six participants who received inhalational sevoflurane anesthesia (male/female: 3/3; age range: 26–62 years) were included. The elective transsphenoidal approach for resection of pituitary microadenoma was used on all participants. An informed written consent was obtained from each participant, and the study was approved by the Ethics Committee of Shanghai Huashan Hospital, Fudan University, Shanghai, China.

We administered 8% sevoflurane in 100% oxygen with a fresh gas flow of 6 L/min to the sevoflurane group, along with remifentanil (1.0 μg/kg) and succinylcholine (1.0 mg/kg). This was maintained with 2.6% (1.3 MAC) ETsevo in 100% oxygen, and a fresh gas flow of 2.0 L/min. Sevoflurane concentration effectively preserved a lack of consciousness in participants identified as ASA physical status I or II. The rest of the anesthesia procedures and the acquisition parameters of fMRI were the same as the Anesthesia group 1.

2.3. Preprocessing

fMRI data was preprocessed using AFNI (Analysis of Functional NeuroImages), including: discarding the first two volumes; slice timing correction; head motion correction; co-registration of functional and structural images; non-linear transformation to Montreal Neurological Institute (MNI) template; a volume and its previous volume were labeled as 0 (or 1, otherwise) if its derivative values of six-dimensional motion parameters have a Euclidean Norm (square root of the sum squares) above 0.5 (Power et al., 2012); band-pass filter was applied between 0.01 and 0.1 Hz; various uninterested components were removed via linear regression, including time series with excessive head motions and their temporal derivatives, mean time series from the white matter and ventricle, and binarized censored time series (output data included zero values at censored time points); spatial smoothing was applied using a Gaussian filter with a full width at half maximum of 6 mm.

2.4. Degree centrality analysis

According to the graph theory, the number of edges connecting a node with other nodes reflects the importance of a node, which is defined as its degree centrality (Oldham and Fornito, 2019). Based on this definition, each voxel in an fMRI image was considered a node, and the functional connection (Pearson correlation of BOLD time series) between the voxel (i.e. node) and any other voxel could be considered an edge. In this study, a binary mask was created using the Human Brainnetome Atlas which includes the grey matter and subcortical regions (Fan et al., 2016), and then a voxel-wise degree centrality map for each participant was generated using the 3dDegreeCentrality program in AFNI. Specifically, we obtained a voxel-wise correlation matrix for each participant by calculating the correlation coefficient between any pair of voxels. This matrix was then binarized by applying a threshold at $r > 0.3$ for each voxel, where an above-threshold correlation coefficient stands for a valid connection, and the degree centrality was calculated as the sum of connections for every voxel. To validate the effect of different thresholds, we also calculated degree centrality maps at $r > 0.2$ and $r > 0.4$ respectively.

To identify cortical regions related to the recovery of consciousness, the degree centrality maps were compared between the UWS-E and UWS-R subgroups. Specifically, an independent samples *t*-test was performed using the 3dttest++ program in AFNI with a cluster-level significance threshold of $p < 0.05$ after FWE correction ($p < 0.005$ uncorrected, cluster size > 91 voxels, 3dClusterSim, AFNI). In this step, patients with mean degree centrality values beyond the range (mean ± 3SD) for each group were considered as an outlier and excluded from further analysis, which resulted in the exclusion of one UWS-E patient and one UWS-R patient. After the comparison, regions with a significant difference of degree centrality values were obtained, which was used as ROIs for further analyses.

Next, to further investigate the relationship between the degree centrality values within the ROIs and the improvement of the patient's ability, partial Spearman correlation between the degree centrality and the patients' GOS scores was calculated, in which the global mean of degree centrality value was treated as a confounding variable. All p values of the spearman correlation coefficient were FDR corrected.

2.5. Comparison of cortical hub distribution between UWS-E and UWS-R

To see whether the same distribution of hubs was maintained in UWS-E and UWS-R, ROIs obtained from the degree centrality analysis were used as masks, and the number of overlapped voxels between these ROIs and the distribution of hubs for each individual participant was calculated. For that we first normalized the degree centrality scores into Z scores with zero mean and unit variance for each individual participant, turning a degree centrality map into a Z score map, where cortical hubs were defined as voxels with z values over 1 (Oldham and Fornito, 2019; Sporns et al., 2007). Next, we calculated the number of overlapped voxels between the ROIs and the hubs found in each individual map for the UWS-E and UWS-R patients respectively. Finally, for each ROI, the numbers of these overlapped voxels for each individual were compared between the two UWS subgroups using independent sample *t*-test. All p values above were FDR corrected.

2.6. Validation of the UWS result with sleep and anesthesia states

First, the group-level spatial distribution of cortical hubs was computed for UWS-E, UWS-R, and all six validation groups (three independent N3 sleep datasets and three independent anesthesia datasets). Specifically, degree centrality maps within each group were averaged and transformed to a Z score map. The cortical hubs for each group were defined in the same way as above, thus creating a binarized map of cortical hubs in each group. Then, the dice coefficient (Dice, 1945) was used to measure the spatial similarity of the binary maps for the cortical hubs between the two groups, which equals two times the number of overlapped voxels divided by the total number of voxels in both binary maps, and has a value that ranges from 0 to 1, in which 1 denotes perfect overlapped voxels and 0 denotes no overlapped voxels (Tie et al., 2014). Within the range of each ROI, a total of 12 dice coefficients were calculated, including six from the pairwise combinations between UWS-E and validation groups, and six from between UWS-R and validation groups. The Mann–Whitney *U* test was then used to compare the difference of dice coefficients. All p values above were FDR corrected.

In the last step, we used the common hub regions identified in the previous steps as seeds, which showed high similarity of hub characteristics among UWS-E, N3 sleep and anesthesia, to calculate the

functional connectivity for all groups, to obtain the connectivity patterns under various unconscious states. For each group, the connectivity pattern was obtained by applying a threshold with a Z value at 0.3095 (r = 0.3). Then the dice coefficient was used again to measure the spatial similarity of the connectivity patterns between UWS-E and validation groups, as well as between UWS-R and validation groups. A permutation test with 10,000 iterations was performed to compare the difference of dice coefficients. In addition, to see the connectivity pattern under the conscious state, the fMRI data of eighty-eight healthy volunteers in their conscious state was obtained (in which 77 came from the participants used for the unconscious state in the validation analysis), and the connectivity pattern was also calculated using the same seeds in the previous step to serve as a reference template.

3. Results

3.1. Cortical regions related to the recovery of consciousness in patients with UWS

Firstly, four cortical regions showed higher degree centrality values in the UWS-E > UWS-R contrast, including the anterior precuneus (PCun), left inferior parietal lobule (LIPL), left inferior frontal gyrus (LIFG), and left middle frontal gyrus (LMFG) (FWE corrected, $p < 0.005$, cluster size > 91 voxels) (Fig. 1A-D, left column). In addition, this result was consistent with different thresholds of $r > 0.2$ or $r > 0.4$. For detailed information about the above four cortical regions and other regions that cannot survive the FWE correction, please see Supplementary Table 2.

Next, partial spearman correlation between the mean degree centrality and GOS scores showed significant positive correlations in the anterior PCun (ρ (23) = 0.59 [95% CI 0.26 to 0.80], $p < 0.01$), LIPL (ρ (23) = 0.51 [95% CI 0.14 to 0.75], $p < 0.05$), LIFG (ρ (23) = 0.55 [95% CI 0.20 to 0.78], $p < 0.01$), and LMFG (ρ (23) = 0.50 [95% CI 0.14 to 0.75], $p < 0.05$) (Fig. 1A-D, right column). All p values were FDR corrected.

3.2. Comparison of cortical hub distribution between UWS-E and UWS-R

As shown in Fig. 2, the group-level spatial distribution of cortical hubs (blue area) and the contour of all four cortical regions obtained in

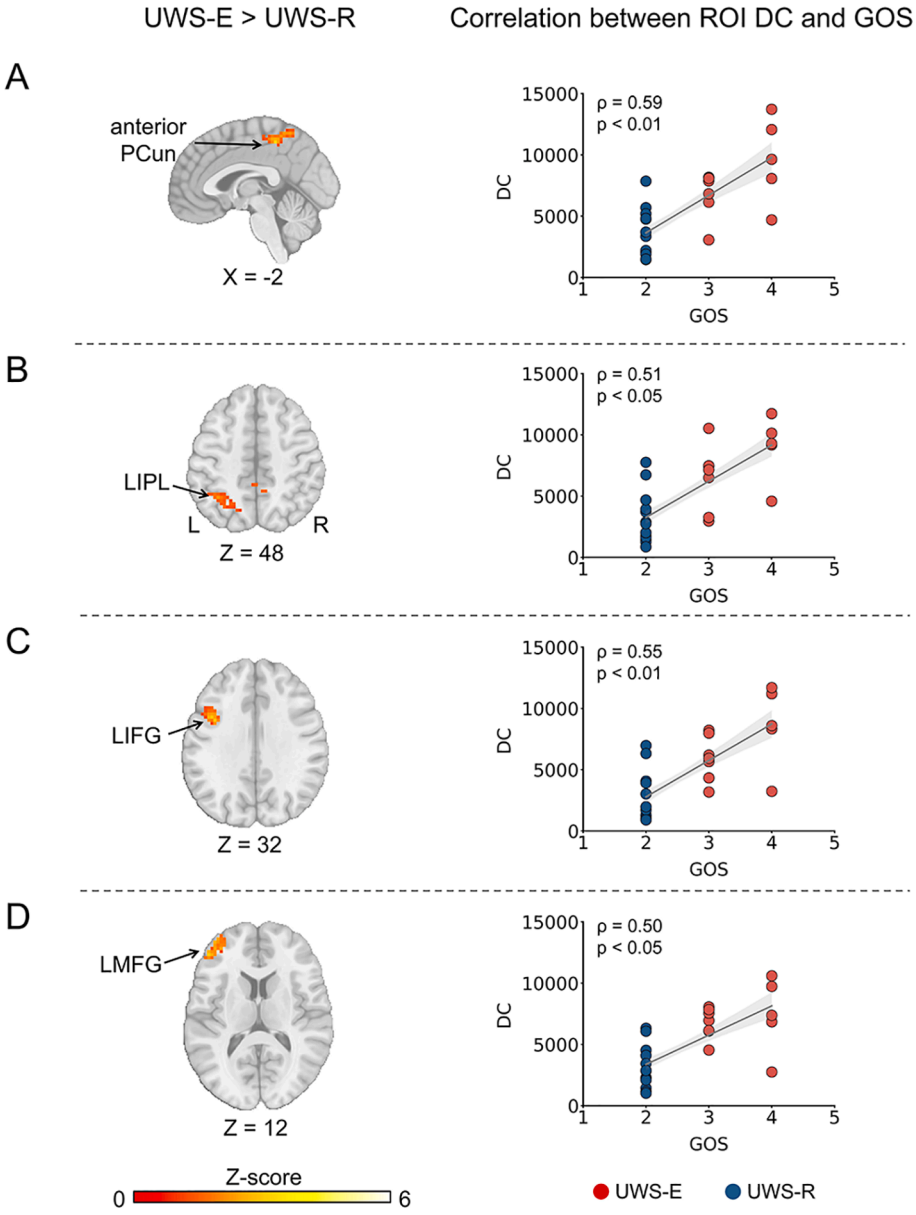

Fig. 1. Cortical regions with increased degree centrality in UWS-E than UWS-R (left column) and their correlation with clinical outcomes (right column). Four cortical regions were obtained including the anterior PCun (A), LIPL (B), LIFG (C), and LMFG (D). PCun = precuneus; LIPL = left inferior parietal lobule; LIFG = left inferior frontal gyrus; LMFG = left middle frontal gyrus; UWS = unresponsive wakefulness syndrome; UWS-E = patients who emerged from UWS at least three months after the experiment performance; UWS-R = patients who remained in UWS at least three months after the experiment performance; DC = degree centrality; GOS = Glasgow Outcome Scale.

the above step (red solid line) were visually displayed for the UWS-E (Fig. 2A-D, left column) and UWS-R (Fig. 2A-D, middle column). In addition, direct comparison between the two subgroups showed significantly more voxels for UWS-E which overlapped with the four cortical regions identified in the above step (Fig. 2A-D, right column).

3.3. Similarity of cortical hub distribution among UWS-E, N3 sleep and anesthesia states

As shown in Fig. 3, the group-level spatial distribution of cortical hub regions (blue area) and the contour of all four cortical regions obtained in the first step (red solid line) were visually displayed for each validation group, the combined-sleep group and combined-anesthesia group, respectively. As shown in Fig. 4, group-level comparison of the dice coefficient showed significantly higher similarity with all six validation groups for UWS-E than UWS-R in the anterior PCun ($p < 0.05$, FDR corrected). In addition, this result was consistent with different thresholds of $r > 0.2$ or $r > 0.4$.

3.4. Similarity of functional connectivity patterns among UWS-E, N3 sleep and anesthesia state

For the connectivity patterns in UWS-E (Fig. 5B) and all six validation groups (Fig. 5D-I), large brain areas within the sensorimotor network (SMN) were functionally connected with the anterior PCun, which is similar as the healthy controls (Fig. 5A). Whereas for UWS-R patients, the functional connectivity with the anterior PCun showed a different pattern (Fig. 5C). This result was further validated with the group-level comparison of the dice coefficient (shown in Fig. 6), which revealed a significantly higher similarity for the UWS-E with the

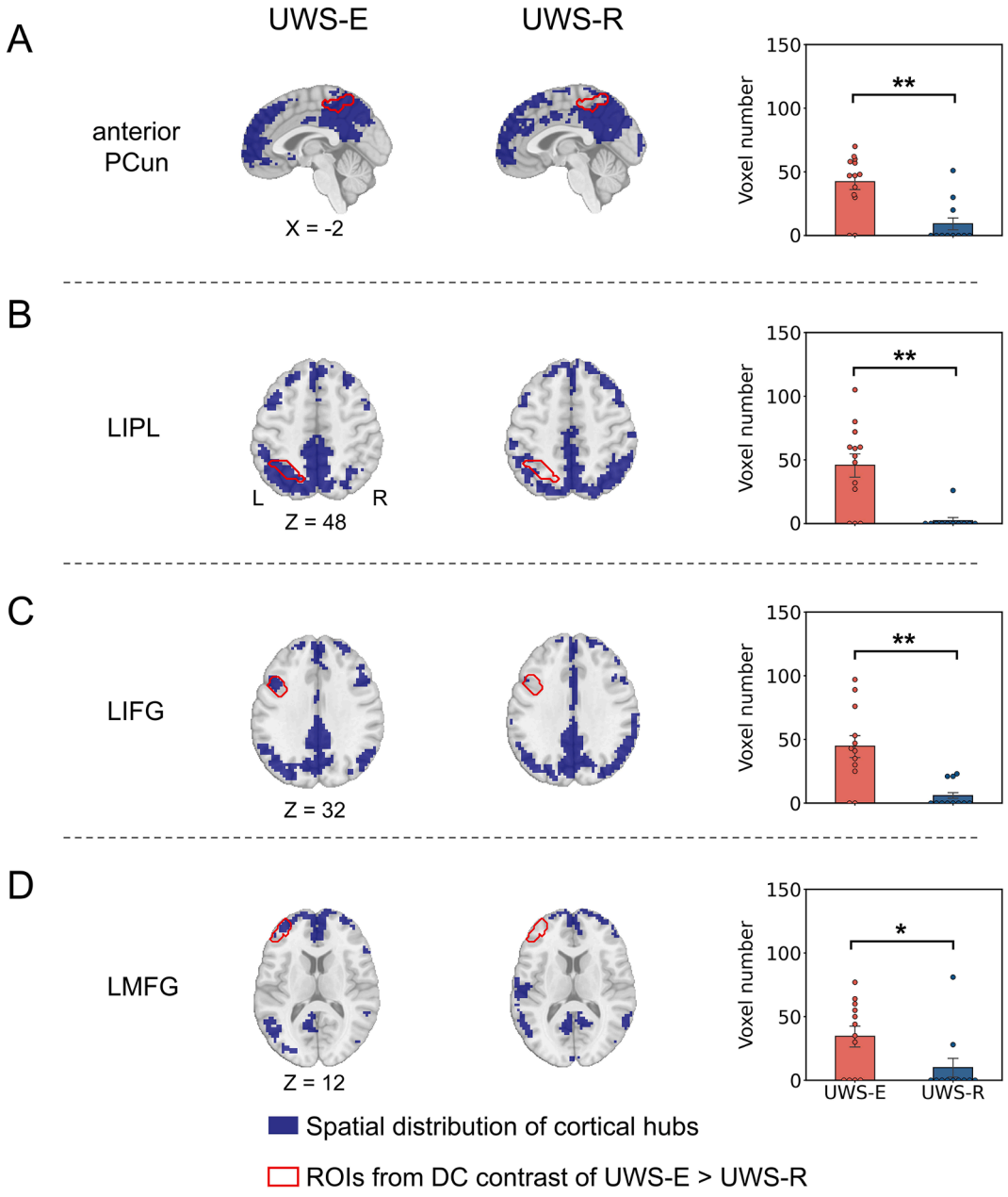

Fig. 2. Comparison of hub distribution in UWS patients. For anterior PCun (A), LIPL (B), LIFG (C) and LMFG (D), the distribution of cortical hubs on a group level (blue area) and the contour of cortical regions obtained from the last step (red solid line) was displayed, as well as the number of overlapped voxels between each ROI and the distribution of hubs for each individual participant was calculated and compared between UWS-E and UWS-R. ** indicates $p < 0.01$ FDR corrected; * indicates $p < 0.05$ FDR corrected. (For interpretation of the references to colour in this figure legend, the reader is referred to the web version of this article.)

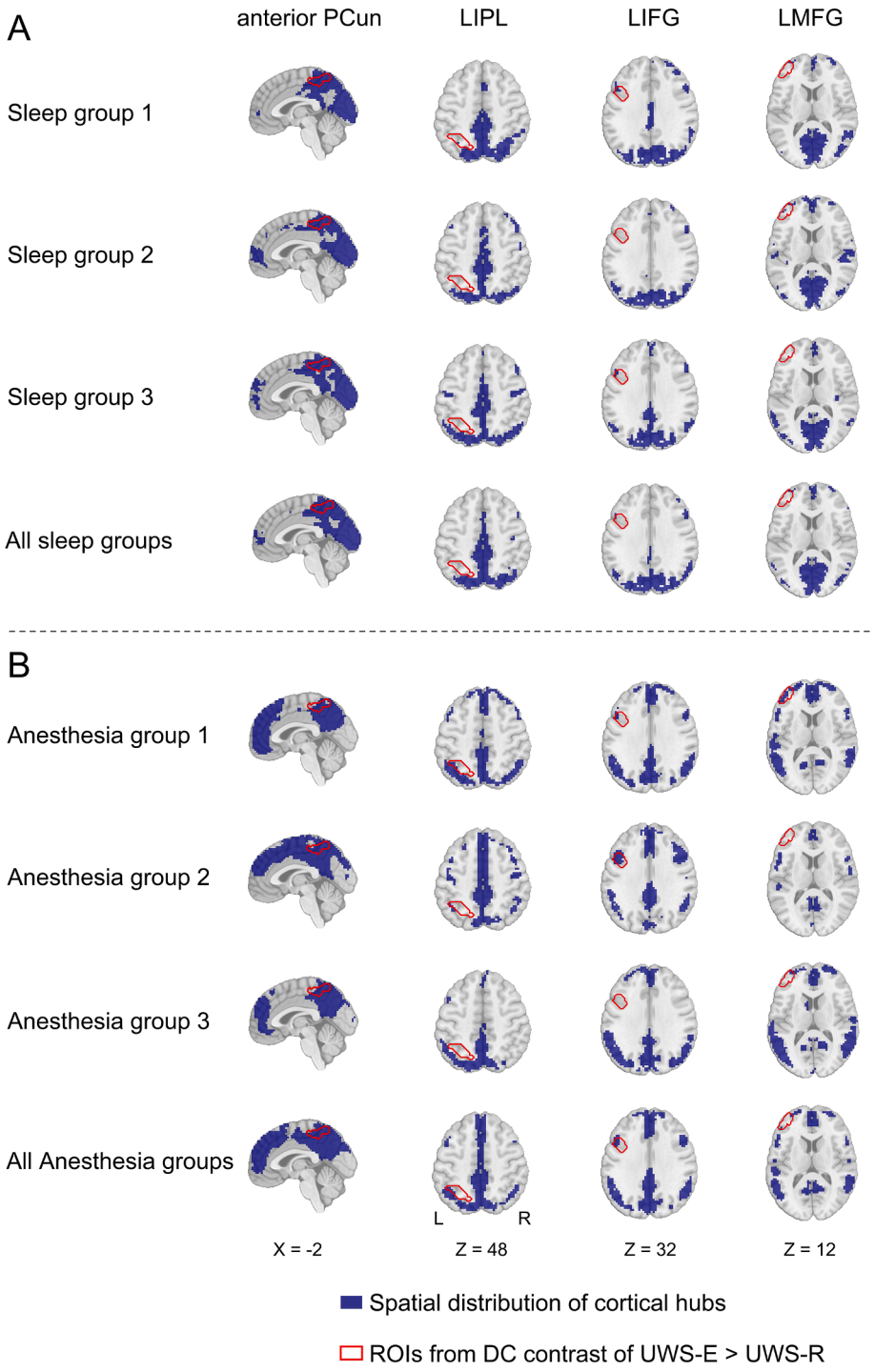

Fig. 3. Spatial distribution of cortical hubs for all validation groups. For each validation group and their combination between sleep (A) and anesthesia (B), the spatial map of cortical hubs (blue area) and the contour of cortical regions obtained from the previous step (red solid line) were presented, for the anterior PCun, LIPL, LIFG, and LMFG (from left to right panels). (For interpretation of the references to colour in this figure legend, the reader is referred to the web version of this article.)

validation groups than UWS-R ($p < 0.05$).

3.5. The functional connectivity between thalamus and four cortical hubs in UWS-E and UWS-R

Considering the important role of thalamus for supporting consciousness (Bastos et al., 2021) and the widespread connection between thalamus and the cortex (Aru et al., 2019), we further tested whether the functional connectivity between thalamus and the cortical hubs (anterior PCun, LIPL, LIFG and LMFG) were different between UWS-E and UWS-R. The results showed that no functional connectivity was different between the UWS-E and UWS-R patients (Supplementary Fig. 1).

4. Discussion

The current study investigates the cortical hubs related to consciousness recovery using patients with UWS. The current study

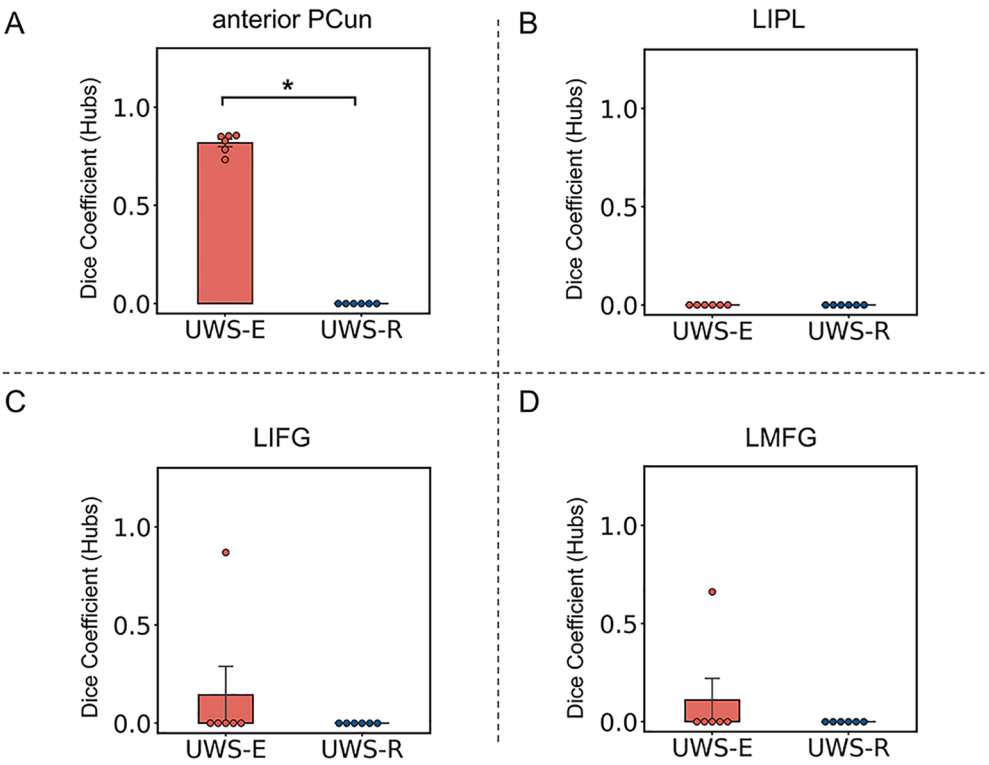

Fig. 4. Spatial similarity of cortical hub distribution between the two patient subgroups and the validation groups. Results of spatial similarity measured with dice coefficient was presented within the anterior PCun (A), LIPL (B), LIFG (C), and LMFG (D). * indicates $p < 0.05$ FDR corrected.

identified four cortical hub regions in the UWS-E, which showed significantly higher degree centrality in UWS-E than UWS-R, including the anterior PCun, LIPL, LIFG and, LMFG. This indicated that differential hub characteristics could discriminate UWS-E and UWS-R patients. Furthermore, among these four hub regions in UWS-E, the anterior PCun consistently showed higher similarity in hub characteristics as well as connectivity patterns, among various recoverable unconscious states, including N3 sleep and anesthesia. Given that the cortical hub regions identified in the current study could distinguish between the patients in UWS who recover consciousness from those who do not, they may serve as potential treatment targets for patients with UWS.

In the current study, the anterior PCun was found to be a hub that could be related to patients' recovery from UWS. This is supported by the previous study indicating that the anterior PCun could play an important role in multisensory information integration, which was found associated with bodily awareness in healthy participants (Herbet et al., 2019). In addition, our findings showed that the anterior PCun had more functional connections to the SMN in UWS-E than in UWS-R. This is in line with previous studies, which found that the anterior PCun was functionally connected to the SMN, and was regarded as a sensorimotor region (Luo et al., 2020; Margulies et al., 2009). In particular, it has been reported that the ability of somatosensory discrimination was found strongly correlated with the UWS patients' clinical outcomes (Spataro et al., 2018), and repetitive transcranial magnetic stimulation (Piccione et al., 2011) and transcranial direct-current stimulation (Angelakis et al., 2014) to the SMN in patients with DOC could cause clinical improvement. The current results provided neural evidence for these findings about relationship between somatosensory and recovery of consciousness in disorders of consciousness.

More interestingly, the current results showed similar hub characteristics and functional connectivity patterns for anterior PCun in all recoverable unconscious states (UWS-E, N3 sleep and anesthesia). Beyond the previous findings that precuneus activity was found preserved or increased during sedation (Liu et al., 2014; Venkatraghavan et al., 2017) and N3 sleep state (Horovitz et al., 2009; Tagliazucchi et al., 2013), our study showed that in conditions where consciousness could be restored (UWS-E, N3 sleep, anesthesia), the connectivity patterns with the anterior PCun was highly similar, which was different from UWS-R. Taken together, the current results indicated that the anterior PCun could be a sensorimotor hub that plays a crucial role in preserving the functional integrity that supports the recovery of consciousness in general.

In the current findings, the LIPL also showed higher degree centrality values for UWS-E than for UWS-R. This finding is consistent with previous literature, which showed that the LIPL connectivity was positively correlated with outcomes in DOC patients (Qin et al., 2015; Zhang et al., 2018). As a key node of the default mode network (DMN), the LIPL was indicated to integrate multisensory information from external pathways including visual, auditory, and somatosensory processing (Wang et al., 2017). Combining the current result, one could assume that a preserved ability of external sensory integration may also be necessary for the recovery of consciousness in DOC patients. On the other hand, our results showed extensive hub distributions within the midline components of DMN for both UWS-E and UWS-R as well as N3 sleep and anesthesia states, which include the posterior cingulate cortex (PCC), ventral precuneus, and medial prefrontal cortex (MPFC). Previous studies also showed that spontaneous synchronized DMN activity was preserved in patients in coma (Norton et al., 2012; Silva et al., 2015), UWS (Boly et al., 2009; Di Perri et al., 2016), N3 sleep stage (Horovitz et al., 2009; Tagliazucchi et al., 2013), as well as in the propofol and sevoflurane-induced sedation (Greicius et al., 2008; Martuzzi et al., 2010; Stamatakis et al., 2010). These findings indicated that different regions of the DMN might have different relationship with the recovery of consciousness.

LMFG and LIFG were also found to be hub regions in UWS-E, but not in N3 sleep and anesthesia states. LMFG and LIFG are regions within the frontoparietal network (FPN). According to the mesocircuit frontoparietal model, the activation of the FPN is strongly associated with the restoration of function within the anterior forebrain mesocircuit, which could support graded reemergence of behavioral responsiveness

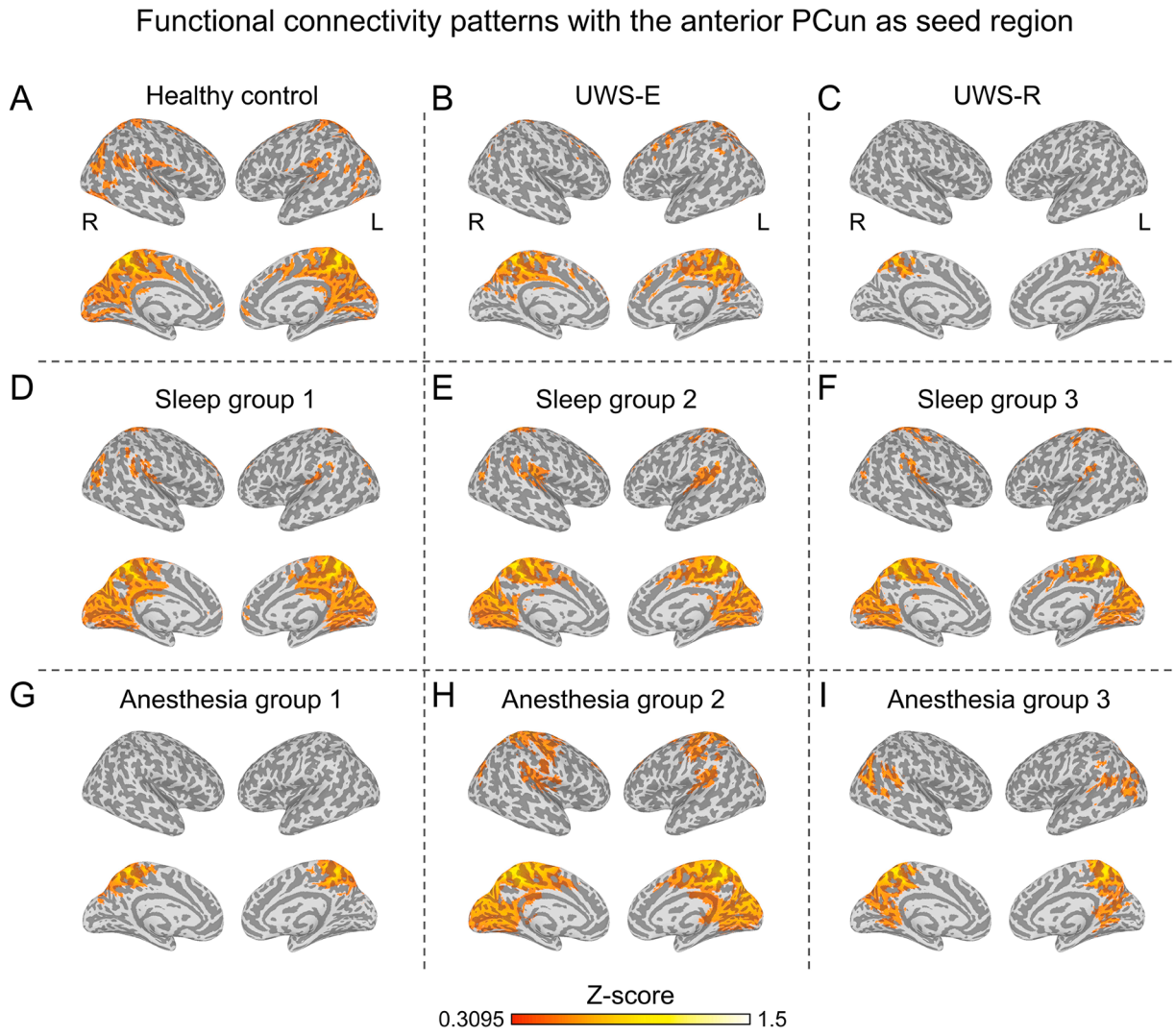

Fig. 5. Functional connectivity of the anterior precuneus. Average functional connectivity map with a threshold at a Z value of 0.3095 was displayed for healthy control group (A), UWS-E (B), UWS-R (C), all three sleep groups (D-F), and all three anesthesia groups (G-I).

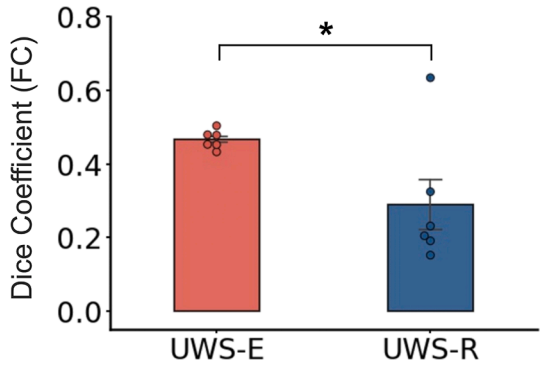

Fig. 6. Comparison of the dice coefficient of the functional connectivity with the anterior precuneus between UWS-E and validation groups, as well as between UWS-R and validation groups. * indicates $p < 0.05$.

across different levels of DOC (Laureys and Schiff, 2012). The current finding supported this model in that the preserved functional integration in the frontal cortex was relevant for consciousness recovery in UWS patients.

The importance of thalamus for supporting consciousness has been widely investigated in previous studies. For example, in multiple unconscious states, including N3 sleep (Guldenmund et al., 2017; Picchioni et al., 2014), anesthesia (Akeju et al., 2014; Guldenmund et al., 2013), and UWS patients (Crone et al., 2014), thalamo-cortical functional connectivity was found disrupted relative to the awake state. Different from the previous studies which focused on the relationship between thalamo-cortical connection and levels of consciousness, the current study tested the connection between the thalamus and the four cortical hubs, which showed higher DC values in UWS patients who had the ability to regain consciousness later. The results showed that none of these connections were different between the UWS-E and UWS-R patients. Taken together, although the thalamus plays an important role in consciousness, the relationship between the thalamus and the recovery of consciousness may need further investigation in the future.

Several issues should be noted, firstly, recent studies showed that 20% of UWS patients had clear brain activation patterns in response to specific active tasks (Cruse et al., 2011; Monti et al., 2010). These patients belong to a condition called cognitive motor dissociation (CMD), who show no detectable command-following behaviors, but show clear neuroimaging evidence of command following brain activities using EEG and fMRI (Schiff, 2015). Since neuroimage or brain-computer interface (BCI) methods (Pan et al., 2020) were not included to identify CMD patients in the current study, we could not rule out the possibility that some UWS patients might be CMD patients, who were

conscious during the period of the experiment performance. Secondly, the Glasgow Outcome Scale for assessing the UWS patients' consciousness recovery was carried out from 3 months to one year after the scanning. However, it is possible that some UWS patients who were regarded as remained in UWS (UWS-R) may need a longer time (more than one year) to regain consciousness, and this could be the reason why a few UWS-R patients showed a similar data pattern (Fig. 1 and Fig. 2) as UWS-E patients.

5. Conclusions

In conclusion, the current results showed that preserved cortical hub regions were relevant to the clinical outcome in UWS patients, including the anterior PCun, LIPL, LIFG and LMFG. More importantly, only the anterior PCun reliably demonstrated hub characteristics and a high similarity among recoverable unconsciousness states, including UWS-E, N3 sleep and anesthesia. This finding shed light on the neural mechanism of the recovery of consciousness in patients with UWS, and provided a new idea for us to understand the neural mechanism of different processes related to consciousness (Aru et al., 2012). Furthermore, the identified cortical hubs could also provide potential treatment targets for patients with UWS.

CRediT authorship contribution statement

Hang Wu: Software, Methodology, Formal analysis, Data Curation, Writing - Original Draft, Writing - Review & Editing, Visualization. **Zengxin Qi:** Investigation. **Xuehai Wu:** Conceptualization, Investigation, Writing - Review & Editing, Funding acquisition. **Jun Zhang:** Investigation. **Changwei Wu:** Investigation. **Zirui Huang:** Investigation. **Di Zang:** Investigation. **Stuart Fogel:** Investigation, Writing - Original Draft. **Sean Tanabe:** Investigation. **Anthony G. Hudetz:** Writing - Original Draft. **Georg Northoff:** Writing - Original Draft, Writing - Review & Editing, Supervision, Funding acquisition. **Ying Mao:** Conceptualization, Methodology, Writing - Review & Editing, Supervision. **Pengmin Qin:** Supervision, Conceptualization, Writing - Original Draft, Writing - Review & Editing, Visualization, Project administration, Funding acquisition.

Acknowledgements

This work was supported by the National Natural Science Foundation of China (31771249 and 31971032), Key Realm R&D Program of Guangzhou (202007030005), the Major Program of the National Social Science Fund of China (18ZDA293), the Basic and Applied Basic Research Foundation of Guangdong Province (2020A1515011250), Key-Area Research and Development Program of Guangdong Province (2018B030340001), Key Realm R&D Program of Guangdong Province (2019B030335001), Shanghai Municipal Science and Technology Major Project (No.2018SHZDZX01 to Y.M).

Appendix A. Supplementary data

Supplementary data to this article can be found online at https://doi.org/10.1016/j.nicl.2022.102951.

References

Achard, S., Delon-Martin, C., Vertes, P.E., Renard, F., Schenck, M., Schneider, F., Heinrich, C., Kremer, S., Bullmore, E.T., 2012. Hubs of brain functional networks are radically reorganized in comatose patients. Proc. Natl. Acad. Sci. U. S. A. 109 (50), 20608–20613. https://doi.org/10.1073/pnas.1208933109.

Akeju, O., Loggia, M.L., Catana, C., Pavone, K.J., Vazquez, R., Rhee, J., Ramirez, V.C., Chonde, D.B., Izquierdo-Garcia, D., Arabasz, G., Hsu, S., Habeeb, K., Hooker, J.M., Napadow, V., Brown, E.N., Purdon, P.L., 2014. Disruption of thalamic functional connectivity is a neural correlate of dexmedetomidine-induced unconsciousness. Elife 3, 1–23. https://doi.org/10.7554/eLife.04499.

Amico, E., Marinazzo, D., Di Perri, C., Heine, L., Annen, J., Martial, C., Dzemidzic, M., Kirsch, M., Bonhomme, V., Laureys, S., Goñi, J., 2017. Mapping the functional connectome traits of levels of consciousness. Neuroimage 148, 201–211. https://doi.org/10.1016/j.neuroimage.2017.01.020.

Angelakis, E., Liouta, E., Andreadis, N., Korfias, S., Ktonas, P., Stranjalis, G., Sakas, D.E., 2014. Transcranial direct current stimulation effects in disorders of consciousness. Arch. Phys. Med. Rehabil. 95 (2), 283–289. https://doi.org/10.1016/j.apmr.2013.09.002.

Aru, J., Bachmann, T., Singer, W., Melloni, L., 2012. Distilling the neural correlates of consciousness. Neurosci. Biobehav. Rev. 36 (2), 737–746. https://doi.org/10.1016/j.neubiorev.2011.12.003.

Aru, J., Suzuki, M., Rutiku, R., Larkum, M.E., Bachmann, T., 2019. Coupling the State and Contents of Consciousness. Front. Syst. Neurosci. 13, 1–9. https://doi.org/10.3389/fnsys.2019.00043.

Bastos, A.M., Donoghue, J.A., Brincat, S.L., Mahnke, M., Yanar, J., Correa, J., Waite, A.S., Lundqvist, M., Roy, J., Brown, E.N., Miller, E.K., 2021. Neural effects of propofol-induced unconsciousness and its reversal using thalamic stimulation. Elife 10, 1–28. https://doi.org/10.7554/ELIFE.60824.

Boly, M., Tshibanda, L., Vanhaudenhuyse, A., Noirhomme, Q., Schnakers, C., Ledoux, D., Boveroux, P., Garweg, C., Lambermont, B., Phillips, C., Luxen, A., Moonen, G., Bassetti, C., Maquet, P., Laureys, S., 2009. Functional connectivity in the default network during resting state is preserved in a vegetative but not in a brain dead patient. Hum. Brain Mapp. 30 (8), 2393–2400. https://doi.org/10.1002/hbm.v30:810.1002/hbm.20672.

Bullmore, E.d., Sporns, O., 2009. Complex brain networks: Graph theoretical analysis of structural and functional systems. Nat. Rev. Neurosci. 10 (3), 186–198. https://doi.org/10.1038/nrn2575.

Crone, J.S., Soddu, A., Höller, Y., Vanhaudenhuyse, A., Schurz, M., Bergmann, J., Schmid, E., Trinka, E., Laureys, S., Kronbichler, M., 2014. Altered network properties of the fronto-parietal network and the thalamus in impaired consciousness. NeuroImage Clin. 4, 240–248. https://doi.org/10.1016/j.nicl.2013.12.005.

Cruse, D., Chennu, S., Chatelle, C., Bekinschtein, T.A., Fernández-Espejo, D., Pickard, J. D., Laureys, S., Owen, A.M., 2011. Bedside detection of awareness in the vegetative state: A cohort study. Lancet 378 (9809), 2088–2094. https://doi.org/10.1016/S0140-6736(11)61224-5.

Di Perri, C., Bahri, M.A., Amico, E., Thibaut, A., Heine, L., Antonopoulos, G., Charland-Verville, V., Wannez, S., Gomez, F., Hustinx, R., Tshibanda, L., Demertzi, A., Soddu, A., Laureys, S., 2016. Neural correlates of consciousness in patients who have emerged from a minimally conscious state: A cross-sectional multimodal imaging study. Lancet Neurol. 15 (8), 830–842. https://doi.org/10.1016/S1474-4422(16)00111-3.

Dice, L.R., 1945. Measures of the Amount of Ecologic Association Between Species Author (s): Lee R. Dice Published by : Ecological Society of America Stable URL : http://www.jstor.org/stable/1932409. Ecology 26, 297–302.

Edlow, B.L., Claassen, J., Schiff, N.D., Greer, D.M., 2020. Recovery from disorders of consciousness: mechanisms, prognosis and emerging therapies. Nat. Rev. Neurol. 17 (3), 135–156. https://doi.org/10.1038/s41582-020-00428-x.

Fan, L., Li, H., Zhuo, J., Zhang, Y.u., Wang, J., Chen, L., Yang, Z., Chu, C., Xie, S., Laird, A.R., Fox, P.T., Eickhoff, S.B., Yu, C., Jiang, T., 2016. The Human Brainnetome Atlas: A New Brain Atlas Based on Connectional Architecture. Cereb. Cortex 26 (8), 3508–3526. https://doi.org/10.1093/cercor/bhw157.

Fang, Z., Ray, L.B., Owen, A.M., Fogel, S.M., 2019. Brain activation time-locked to sleep spindles associated with human cognitive abilities. Front. Neurosci. 13, 1–16. https://doi.org/10.3389/fnins.2019.00046.

Fogel, S., Albouy, G., King, B.R., Lungu, O., Vien, C., Bore, A., Pinsard, B., Benali, H., Carrier, J., Doyon, J., Sakakibara, M., 2017. Reactivation or transformation? Motor memory consolidation associated with cerebral activation time-locked to sleep spindles. PLoS One 12 (4), e0174755. https://doi.org/10.1371/journal.pone.0174755.

Giacino, J.T., Fins, J.J., Laureys, S., Schiff, N.D., 2014. Disorders of consciousness after acquired brain injury: The state of the science. Nat. Rev. Neurol. 10 (2), 99–114. https://doi.org/10.1038/nrneurol.2013.279.

Giacino, J.T., Kalmar, K., Whyte, J., 2004. The JFK Coma Recovery Scale-Revised: Measurement characteristics and diagnostic utility. Arch. Phys. Med. Rehabil. 85, 2020–2029. https://doi.org/10.1016/j.apmr.2004.02.033.

Greicius, M.D., Kiviniemi, V., Tervonen, O., Vainionpää, V., Alahuhta, S., Reiss, A.L., Menon, V., 2008. Persistent default-mode network connectivity during light sedation. Hum. Brain Mapp. 29 (7), 839–847. https://doi.org/10.1002/hbm.20537.

Guldenmund, P., Demertzi, A., Boveroux, P., Boly, M., Vanhaudenhuyse, A., Bruno, M.-A., Gosseries, O., Noirhomme, Q., Brichant, J.-F., Bonhomme, V., Laureys, S., Soddu, A., 2013. Thalamus, Brainstem and Salience Network Connectivity Changes During Propofol-Induced Sedation and Unconsciousness. Brain Connect. 3 (3), 273–285. https://doi.org/10.1089/brain.2012.0117.

Guldenmund, P., Vanhaudenhuyse, A., Sanders, R.D., Sleigh, J., Bruno, M.A., Demertzi, A., Bahri, M.A., Jaquet, O., Sanfilippo, J., Baquero, K., Boly, M., Brichant, J.F., Laureys, S., Bonhomme, V., 2017. Brain functional connectivity differentiates dexmedetomidine from propofol and natural sleep. Br. J. Anaesth. 119 (4), 674–684. https://doi.org/10.1093/bja/aex257.

Herbet, G., Lemaitre, A.L., Moritz-Gasser, S., Cochereau, J., Duffau, H., 2019. The antero-dorsal precuneal cortex supports specific aspects of bodily awareness. Brain 142, 2207–2214. https://doi.org/10.1093/brain/awz179.

Heuvel, M.P.V., Van Den, Sporns, S., 2011. Rich-Club Organization of the Human Connectome. J. Neurosci. 31, 15775–15786. https://doi.org/10.1523/JNEUROSCI.3539-11.2011.

Horovitz, S.G., Braun, A.R., Carr, W.S., Picchioni, D., Balkin, T.J., Fukunaga, M., Duyn, J. H., 2009. Decoupling of the brain's default mode network during deep sleep. Proc. Natl. Acad. Sci. U. S. A. 106 (27), 11376–11381. https://doi.org/10.1073/pnas.0901435106.

Huang, Z., Wang, Z., Zhang, J., Dai, R., Wu, J., Li, Y., Liang, W., Mao, Y., Yang, Z., Holland, G., Zhang, J., Northoff, G., 2014. Altered temporal variance and neural synchronization of spontaneous brain activity in anesthesia. Hum. Brain Mapp. 35 (11), 5368–5378. https://doi.org/10.1002/hbm.22556.

Laureys, S., Celesia, G.G., Cohadon, F., Lavrijsen, J., León-Carrión, J., Sannita, W.G., Sazbon, L., Schmutzhard, E., von Wild, K.R., Zeman, A., Dolce, G., 2010. Unresponsive wakefulness syndrome: A new name for the vegetative state or apallic syndrome. BMC Med. 8, 2–5. https://doi.org/10.1186/1741-7015-8-68.

Laureys, S., Schiff, N.D., 2012. Coma and consciousness: Paradigms (re)framed by neuroimaging. Neuroimage 61 (2), 478–491. https://doi.org/10.1016/j.neuroimage.2011.12.041.

Liu, X., Lauer, K.K., Douglas Ward, B., Roberts, C., Liu, S., Gollapudy, S., Rohloff, R., Gross, W., Chen, G., Xu, Z., Binder, J.R., Li, S.J., Hudetz, A.G., 2017. Propofol attenuates low-frequency fluctuations of resting-state fMRI BOLD signal in the anterior frontal cortex upon loss of consciousness. Neuroimage 147, 295–301. https://doi.org/10.1016/j.neuroimage.2016.12.043.

Liu, X., Li, S.J., Hudetz, A.G., 2014. Increased precuneus connectivity during propofol sedation. Neurosci. Lett. 561, 18–23. https://doi.org/10.1016/j.neulet.2013.12.047.

Luo, Z., Zeng, L.L., Qin, J., Hou, C., Shen, H., Hu, D., 2020. Functional Parcellation of Human Brain Precuneus Using Density-Based Clustering. Cereb. Cortex 30, 269–282. https://doi.org/10.1093/cercor/bhz086.

Luppi, A.I., Craig, M.M., Pappas, I., Finoia, P., Williams, G.B., Allanson, J., Pickard, J.D., Owen, A.M., Naci, L., Menon, D.K., Stamatakis, E.A., 2019. Consciousness-specific dynamic interactions of brain integration and functional diversity. Nat. Commun. 10, 4616. https://doi.org/10.1038/s41467-019-12658-9.

Malagurski, B., Péran, P., Sarton, B., Vinour, H., Naboulsi, E., Riu, B., Bounes, F., Seguin, T., Lotterie, J.A., Fourcade, O., Minville, V., Ferré, F., Achard, S., Silva, S., 2019. Topological disintegration of resting state functional connectomes in coma. Neuroimage 195, 354–361. https://doi.org/10.1016/j.neuroimage.2019.03.012.

Margulies, D.S., Vincent, J.L., Kelly, C., Lohmann, G., Uddin, L.Q., Biswal, B.B., Villringer, A., Castellanos, F.X., Milham, M.P., Petrides, M., 2009. Precuneus shares intrinsic functional architecture in humans and monkeys. Proc. Natl. Acad. Sci. U. S. A. 106 (47), 20069–20074. https://doi.org/10.1073/pnas.0905314106.

Martuzzi, R., Ramani, R., Qiu, M., Rajeevan, N., Constable, R.T., 2010. Functional connectivity and alterations in baseline brain state in humans. Neuroimage 49 (1), 823–834. https://doi.org/10.1016/j.neuroimage.2009.07.028.

Monti, M.M., Vanhaudenhuyse, A., Coleman, M.R., Boly, M., Pickard, J.D., Tshibanda, L., Owen, A.M., Laureys, S., 2010. Willful Modulation of Brain Activity in Disorders of Consciousness. N. Engl. J. Med. 362 (7), 579–589. https://doi.org/10.1056/NEJMoa0905370.

Northoff, G., Huang, Z., 2017. How do the brain's time and space mediate consciousness and its different dimensions? Temporo-spatial theory of consciousness (TTC). Neurosci. Biobehav. Rev. 80, 630–645. https://doi.org/10.1016/j.neubiorev.2017.07.013.

Northoff, G., Lamme, V., 2020. Neural signs and mechanisms of consciousness: Is there a potential convergence of theories of consciousness in sight? Neurosci. Biobehav. Rev. 118, 568–587. https://doi.org/10.1016/j.neubiorev.2020.07.019.

Norton, L., Hutchison, R.M., Young, G.B., Lee, D.H., Sharpe, M.D., Mirsattari, S.M., 2012. Disruptions of functional connectivity in the default mode network of comatose patients. Neurology 78 (3), 175–181. https://doi.org/10.1212/WNL.0b013e31823fcd61.

Oldham, S., Fornito, A., 2019. The development of brain network hubs. Dev. Cogn. Neurosci. 36, 100607. https://doi.org/10.1016/j.dcn.2018.12.005.

Pan, J., Xie, Q., Qin, P., Chen, Y., He, Y., Huang, H., Wang, F., Ni, X., Cichocki, A., Yu, R., Li, Y., 2020. Prognosis for patients with cognitive motor dissociation identified by brain-computer interface. Brain 143, 1177–1189. https://doi.org/10.1093/brain/awaa026.

Picchioni, D., Pixa, M.L., Fukunaga, M., Carr, W.S., Horovitz, S.G., Braun, A.R., Duyn, J. H., 2014. Decreased connectivity between the thalamus and the neocortex during human nonrapid eye movement sleep. Sleep 37, 387–397. https://doi.org/10.5665/sleep.3422.

Piccione, F., Cavinato, M., Manganotti, P., Formaggio, E., Storti, S.F., Battistin, L., Cagnin, A., Tonin, P., Dam, M., 2011. Behavioral and neurophysiological effects of repetitive transcranial magnetic stimulation on the minimally conscious state: A case study. Neurorehabil. Neural Repair 25 (1), 98–102. https://doi.org/10.1177/1545968310369802.

Power, J.D., Barnes, K.A., Snyder, A.Z., Schlaggar, B.L., Petersen, S.E., 2012. Spurious but systematic correlations in functional connectivity MRI networks arise from subject motion. Neuroimage 59 (3), 2142–2154. https://doi.org/10.1016/j.neuroimage.2011.10.018.

Qin, P., Wu, X., Wu, C., Wu, H., Zhang, J., Huang, Z., Weng, X., Zang, D., Qi, Z., Tang, W., Hiromi, T., Tan, J., Tanabe, S., Fogel, S., Hudetz, A.G., Yang, Y., Stamatakis, E.A., Mao, Y., Northoff, G., 2021. Higher-order sensorimotor circuit of the brain's global network supports human consciousness. Neuroimage 231, 117850. https://doi.org/10.1016/j.neuroimage.2021.117850.

Qin, P., Wu, X., Huang, Z., Duncan, N.W., Tang, W., Wolff, A., Hu, J., Gao, L., Jin, Y., Wu, X., Zhang, J., Lu, L., Wu, C., Qu, X., Mao, Y., Weng, X., Zhang, J., Northoff, G., 2015. How are different neural networks related to consciousness? Ann. Neurol. 78 (4), 594–605. https://doi.org/10.1002/ana.24479.

Rosazza, C., Andronache, A., Sattin, D., Bruzzone, M.G., Marotta, G., Nigri, A., Ferraro, S., Rossi Sebastiano, D., Porcu, L., Bersano, A., Benti, R., Leonardi, M., D'Incerti, L., Minati, L., 2016. Multimodal study of default-mode network integrity in disorders of consciousness. Ann. Neurol. 79 (5), 841–853. https://doi.org/10.1002/ana.24634.

Schiff, N.D., 2015. Cognitive motor dissociation following severe brain injuries. JAMA Neurol. 72, 1413–1415. https://doi.org/10.1001/jamaneurol.2015.2899.

Silva, S., de Pasquale, F., Vuillaume, C., Riu, B., Loubinoux, I., Geeraerts, T., Seguin, T., Bounes, V., Fourcade, O., Demonet, J.-F., Péran, P., 2015. Disruption of posteromedial large-scale neural communication predicts recovery from coma. Neurology 85, 2036–2044. https://doi.org/10.1212/WNL.0000000000002853.

Song, M., Yang, Y., He, J., Yang, Z., Yu, S., Xie, Q., Xia, X., Dang, Y., Zhang, Q., Wu, X., Cui, Y., Hou, B., Yu, R., Xu, R., Jiang, T., 2018. Prognostication of chronic disorders of consciousness using brain functional networks and clinical characteristics. Elife 7, e36173. https://doi.org/10.7554/eLife.36173.

Spataro, R., Heilinger, A., Allison, B., De Cicco, D., Marchese, S., Gregoretti, C., La Bella, V., Guger, C., 2018. Preserved somatosensory discrimination predicts consciousness recovery in unresponsive wakefulness syndrome. Clin. Neurophysiol. 129 (6), 1130–1136. https://doi.org/10.1016/j.clinph.2018.02.131.

Sporns, O., Honey, C.J., Kötter, R., Kaiser, M., 2007. Identification and classification of hubs in brain networks. PLoS One 2 (10), e1049. https://doi.org/10.1371/journal.pone.0001049.

Stamatakis, E.A., Adapa, R.M., Absalom, A.R., Menon, D.K., Sporns, O., 2010. Changes in resting neural connectivity during propofol sedation. PLoS One 5 (12), e14224. https://doi.org/10.1371/journal.pone.0014224.

Tagliazucchi, E., von Wegner, F., Morzelewski, A., Brodbeck, V., Borisov, S., Jahnke, K., Laufs, H., 2013. Large-scale brain functional modularity is reflected in slow electroencephalographic rhythms across the human non-rapid eye movement sleep cycle. Neuroimage 70, 327–339. https://doi.org/10.1016/j.neuroimage.2012.12.073.

Tie, Y., Rigolo, L., Norton, I.H., Huang, R.Y., Wu, W., Orringer, D., Mukundan, S., Golby, A.J., 2014. Defining language networks from resting-state fMRI for surgical planning- A feasibility study. Hum. Brain Mapp. 35 (3), 1018–1030. https://doi.org/10.1002/hbm.22231.

Tsai, P.J., Chen, S.C.J., Hsu, C.Y., Wu, C.W., Wu, Y.C., Hung, C.S., Yang, A.C., Liu, P.Y., Biswal, B., Lin, C.P., 2014. Local awakening: Regional reorganizations of brain oscillations after sleep. Neuroimage 102, 894–903. https://doi.org/10.1016/j.neuroimage.2014.07.032.

Venkatraghavan, L., Bharadwaj, S., Wourms, V., Tan, A., Jurkiewicz, M.T., Mikulis, D.J., Crawley, A.P., 2017. Brain Resting-State Functional Connectivity Is Preserved under Sevoflurane Anesthesia in Patients with Pervasive Developmental Disorders: A Pilot Study. Brain Connect. 7 (4), 250–257. https://doi.org/10.1089/brain.2016.0448.

Wang, J., Xie, S., Guo, X., Becker, B., Fox, P.T., Eickhoff, S.B., Jiang, T., 2017. Correspondent Functional Topography of the Human Left Inferior Parietal Lobule at Rest and Under Task Revealed Using Resting-State fMRI and Coactivation Based Parcellation. Hum. Brain Mapp. 38 (3), 1659–1675. https://doi.org/10.1002/hbm.23488.

Wang, J.-H., Zuo, X.-N., Gohel, S., Milham, M.P., Biswal, B.B., He, Y., Kaiser, M., 2011. Graph theoretical analysis of functional brain networks: Test-retest evaluation on short- and long-term resting-state functional MRI data. PLoS One 6 (7), e21976. https://doi.org/10.1371/journal.pone.0021976.

Zhang, L., Luo, L., Zhou, Z., Xu, K., Zhang, L., Liu, X., Tan, X., Zhang, J., Ye, X., Gao, J., Luo, B., 2018. Functional connectivity of anterior insula predicts recovery of patients with disorders of consciousness. Front. Neurol. 9, 1–10. https://doi.org/10.3389/fneur.2018.01024.